Shared Spectrum Throughput for Secondary Users

Pratik Gandhi   *Pratik_Gandhi1@student.uml.edu*
PhD student/ECE
University of Massachusetts Lowell
Lowell MA, 01854, USA

Kavitha Chandra   *Kavitha_Chandra@uml.edu*
Faculty/ ECE
University of Massachusetts Lowell
Lowell MA, 01854, USA

Charles Thompson   *Charles_Thompson@uml.edu*
Faculty/ ECE
University of Massachusetts Lowell
Lowell MA, 01854, USA

Abstract

The throughput performance of secondary users sharing radio spectrum with a licensed primary user is analyzed in this work. An asynchronous transmission, sensing and backoff protocol is proposed for the secondary user and modeled as a six state Markov process. The model parameters are derived as a function of the duty cycle and average duration that the channel is unoccupied by the primary user. The secondary user parameters include its continuous transmission duration or packet size and its backoff window size. The model results show that the probabilities of the secondary user being in the transmit state are relatively invariant to the duty cycle compared to the probability of being in the backoff state, particularly at low to moderate secondary packet sizes. The secondary user throughput is expressed as a function of the aforementioned parameters and shown to change significantly with duty cycle and secondary packet sizes. It is found that at very low duty cycles, the throughput variation is insensitive to backoff duration being random or fixed. The proposed transmission and sensing method is also shown to outperform a periodic sensing protocol. The regions of the parameter space wherein the backoff and retransmit probabilities of the secondary user are bounded by specified performance metrics are derived. The sensitivity of the throughput in the presence of a cooperative and non-cooperative secondary user is also investigated.

Keywords: Spectrum Sharing, Cognitive Radio, Throughput, Licensed Users, Secondary Users.

1. INTRODUCTION

Radio spectrum sharing between the licensed primary users (PU) also referred as incumbents and opportunistic secondary users (SU) has been examined from various performance, regulation and policy perspectives.   Currently, the executive office of the President's spectrum management team, the Federal Communication Commission (FCC) and the National Telecommunications and Information Administration are evaluating the feasibility of releasing spectrum in the 1695-1710, 1755-1850, 5350-5470 and 5850-5925 MHz bands for secondary usage [1]. The 2012 report [2] to the President from his council of advisors on science and technology recommended identification of 1000 MHz of Federal spectrum for sharing as well as a policy change from auctioning to sharing underutilized spectrum to the maximum extent consistent with the Federal mission. The report makes a strong case for migrating from an exclusive spectrum rights to a shared resource policy, one where novel approaches to spectrum management can lead to a more uniform utilization of the radio spectrum. To evaluate the effectiveness and potential advantage of spectrum sharing, the tradeoff between tolerable interference to PUs and capacity

available for SUs should be understood, taking into consideration the diverse parameters governing frequency bands, transmission and receiver characteristics.

Dynamic spectrum allocation (DSA) has been investigated in the context of spectrum sensing with cognitive radios [3][4][5] and through the use of geolocation databases to detect primary users [6][7][8]. The IEEE 802.22 [9] standard designed for sharing the whitespace generated by transition to digital TV recommends that SUs determine channel availability by querying a database that records the activity of the licensed users at required space and time instants. The decision to use a database driven approach was the result of concerns by the FCC on the harmful interference that could result from the uncertainty of sensing based decisions. The standard however includes allowance for a quiet period during which the SU suspends operation and the physical layer performs channel sensing. Spectrum sensing and database query to identify the presence of the primary user can be construed as two extreme approaches, the former operating with minimal knowledge about the PU and the latter assuming complete knowledge. To enable a more elastic spectrum utilization model, one that accommodates primary users that may operate on a random access basis, it is important to identify those access parameters that have the most impact on the spectrum sharing paradigm. These parameters may be drawn from across the layers of the primary user communications stack and applied to better understand how knowledge of the primary user behavior by cognitive radios can help optimize the coexistence of secondary users and primary transmissions. In [10], a channel sensing scheme based on primary users channel access pattern was found to result in lower ideal channel search delay and higher performance compared to the random channel sensing scheme. Wang *et al.* [11] show the importance of observing PU's on-off behavior to make a prediction about channel availability to achieve higher secondary throughput. Analysis of protocol and parameter compatibility between primary and secondary users can lead regulators to make well-informed decisions on which the under-utilized licensed applications and bands may be suitable for spectrum sharing.

The duty cycle that characterizes the channel usage of a primary user is recognized as an important parameter that governs the viability of a particular licensed band for spectrum sharing. Chang *et al.* [12] show that even with a duty cycle as high as fifty percent, the spectrum sensing performance using energy, waveform and cyclostationary detection degrades significantly. However, primary users with low duty cycles are expected to be good candidates for sharing spectrum and therefore efficient methods to identify and utilize the durations when PUs are not occupying the channel are quite important. Gabran *et al.* [13] presented methods for the joint estimation of the primary user traffic parameters, including the average duty cycle and quantified the estimation error and its impact on spectrum sensing performance. Kim and Shin [14] investigated sensing at the medium access control (MAC) layer and showed that the sensing duration could be optimized to maximally identify available spectrum considering the probability distributions of the on-off alternating renewal processes that characterized the PU activity. The application of a cross-layer approach, beginning with joint MAC and physical layer functions has the potential to afford significant spectrum sharing gains. Zheng *et al.* [15] compare the throughput performance of SU's for both the layered and cross-layered approaches and show that the SU throughput is nearly doubled when spectrum sensing at the physical layer is integrated with the medium access protocol at the higher layer. A survey of medium access protocols for cognitive radios (CR) is given in [16], where random access, time slotted and hybrid MAC protocols are classified for cognitive radio infrastructure-based and ad hoc networks. The optimization of spectrum sensing and transmission duration so as to maximize the SU throughput while minimizing interference to the PU is the key objective of CR-MAC protocols. Previous work in this area has considered finding the optimal operating region for transmission and sensing times as a function of the probability of PU being on or off [17], optimizing transmission duration while keeping the sensing period fixed [18] or finding the optimum sensing period given a fixed transmission duration [19].

The work presented here demonstrates operating regions considering both PU and SU access parameters. In particular, it determines how small the PU duty cycle has to be to obtain a useful

SU throughput and how the transmission window size of the SU affects the system performance. The channel sharing is analyzed assuming complete knowledge of the PU access patterns, which is assumed to be an on-off Markov chain. The SU access pattern with the knowledge of PU parameters is represented by a six state Markov chain and includes the functions of spectrum sensing, transmission and backoff when the channel is occupied. This approach is shown to provide the optimal SU transmission frame sizes, corresponding throughput and operating regions based on performance specifications that bounding the probabilities of SU occupying backoff, transmit and retransmit states.

Section 2 presents a MAC layer model for the secondary users considering a fixed backoff window and derives the SU state probabilities for a range of PU duty cycles. The SU throughput is derived in Section 3. Section 4 compares the model with results from simulation. The effect of randomly distributed backoff windows on the SU throughput is presented in Section 5. The performance with two secondary users is analyzed in Sections 6 and 7 assuming the case of a cooperative and a non-cooperative user respectively. Section 8 concludes the paper.

2. TIME-SLOTTED MAC LAYER MODEL FOR THROUGHPUT OF SECONDARY USERS

The PU channel usage is described using a two state discrete time Markov chain X_n, n=1, 2… where n is the slotted time index. The two states referred as on and off states represent respectively, the times when the PU is utilizing the spectrum or when the channel is available for sharing. The average durations of the on and off periods are represented by T_{on} and T_{off} respectively. The PU changes from the on to off state with probability β and from the off to on state with probability α. Assuming that the on and off durations are represented as geometrically distributed random variables, the average on and off periods are related to the transition probabilities as $T_{on} = 1/\beta$ and $T_{off} = 1/\alpha$. Of interest are the average duty cycle of the PU $D_c = T_{on}/(T_{on} + T_{off}) = \alpha/(\alpha + \beta)$ and the sensitivity of the SU throughput performance to this parameter.

The SU model presented here extends the authors' previous work [20] on modeling sensing and transmission probabilities to include a theoretical analysis of the SU throughput performance, randomly distributed backoff window sizes and the performance impact of non-cooperative secondary users. The model that approximates a MAC layer function includes transmission, backoff and channel sensing states. The sensing state incorporates information communicated from the PHY layer on channel availability at the requested time-slot. The objective is to determine an optimal operating space delineated by the PU parameters, $D_c(\alpha, \beta)$, the backoff window bwin, the SU transmission duration or packet size S_p and the throughput R_T. A continuous stream of SU transmission frames is assumed to be queued and available, thus operating in what is referred as a saturation mode. It is also assumed that no packets are dropped and as many retransmissions necessary for an error-free transmission are carried out, thus providing an upper bound to the delay experienced by an opportunistic SU.
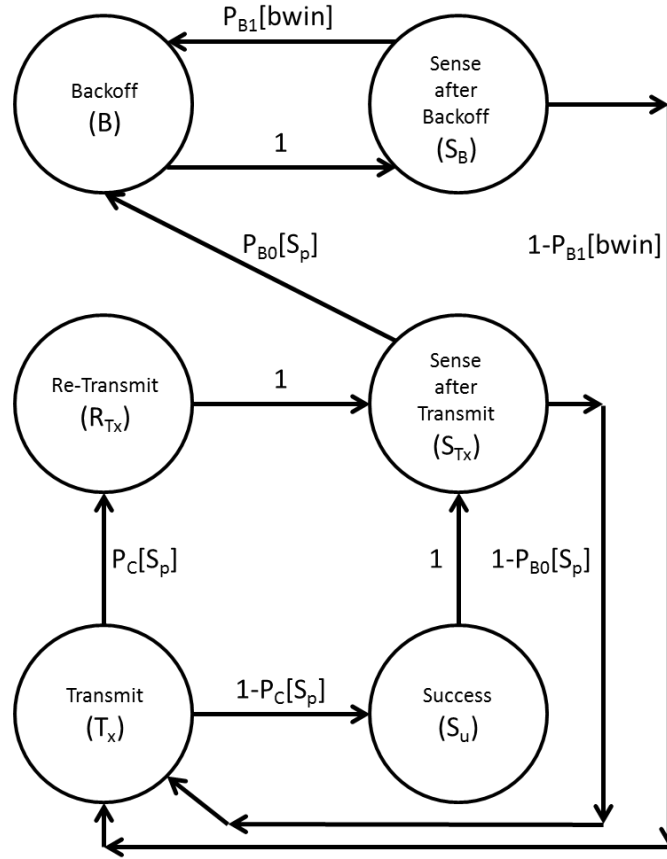
FIGURE 1: MAC Layer State Transition Diagram.

The SU behavior is represented by a six state Markov model that is shown in Fig. 1 and represented by the process Y_n, n=1, 2.... The two sensing states S_{T_x}, S_B record the channel status after completing a transmission or backoff respectively. During the transmit state, the SU is unable to sense the channel, but on completion the likelihood of a collision with the PU can be determined. If the PU accessed the channel during the T_x state, based on the number of time-slots involved in the collision, the SU will either enter the retransmit (R_{T_x}) state and sense the channel (S_{T_x}) before transmitting or complete a successful transmission through the S_u state. The respective transition probabilities can be tuned to take into account any error-correcting resilience in the SU and/or PU transmission protocols.

The transition probabilities for the MAC layer model are derived from the PU on-off process. The probabilities $P_{B0}[k]$ and $P_{B1}[k]$ represent the conditional probabilities of the channel being busy after k+1 time slots starting from an idle state and starting from a busy state respectively. The probability $P_C[k]$ represents the probability of collision with the secondary in at least one time slot during the transmission period. The ability to tolerate collisions in more than one time slot can also be accommodated through this parameter.

The transmission frame length is represented as S_p discrete time units. If one or more collisions are experienced by the SU packet during the transmission state, the process enters the retransmit state R_{T_x} with probability $P_C[S_p]$, otherwise it enters the success state S_u with probability $1 - P_C[S_p]$, followed by the channel sense state S_{T_x}. On obtaining information from the PHY layer, if the channel is busy, the process enters the backoff state B with probability $P_{B0}[S_p]$ for a period $bwin$. The sense after backoff state S_B is entered after $bwin$ time periods. Retrieving

channel information from the PHY layer, if the channel is busy, the system backs off with probability $P_{B1}[bwin]$. If the channel is free the packet transmit state is initiated with probability $1 - P_{B1}[bwin]$. The state transition matrix P_Y, representing the SU dynamics is given as,

$$
\begin{array}{c}
\begin{array}{cccccc}
\quad B & S_B & T_x & S_{T_x} & R_{T_x} & S_u
\end{array} \\
\begin{array}{c}
B \\
S_B \\
T_x \\
S_{T_x} \\
R_{T_x} \\
S_u
\end{array}
\left(
\begin{array}{cccccc}
0 & 1 & 0 & 0 & 0 & 0 \\
P_{B1}[bwin] & 0 & 1 - P_{B1}[bwin] & 0 & 0 & 0 \\
0 & 0 & 0 & 0 & P_C[S_p] & 1 - P_C[S_p] \\
P_{B0}[S_p] & 0 & 1 - P_{B0}[S_p] & 0 & 0 & 0 \\
0 & 0 & 0 & 1 & 0 & 0 \\
0 & 0 & 0 & 1 & 0 & 0
\end{array}
\right)
\end{array}
\tag{1}
$$

The state S_u representing successful packet transmission is introduced here to distinguish entry into the sense after transmit (S_{T_x}) state after a successful packet transmission or through retransmit (R_{T_x}) state after a collision with the primary. The two sensing states, allow the evaluation of suitable ($S_p, bwin$) parameters for a particular PU duty cycle.

The transition probabilities, $P_C[S_p]$, $P_{B0}[S_p]$, $P_{B1}[bwin]$ are derived from the two state Markov chain descriptor of the primary channel [21]. The n-step transition probability matrix for the PU with elements $(p_{ij})^n$ representing the probability of transition from state i to state j in n steps is as follows:

$$
\mathbf{P}_X^n = \frac{1}{\alpha + \beta} \begin{bmatrix} \beta + \alpha(1 - \alpha - \beta)^n & \alpha(1 - (1 - \alpha - \beta)^n) \\ \beta(1 - (1 - \alpha - \beta)^n) & \alpha + \beta(1 - \alpha - \beta)^n \end{bmatrix}
\tag{2}
$$

With respect to D_c, the transition probabilities $P_{B0}[S_p]$ and $P_{B1}[bwin]$ are given as,

$$
P_{B0}[S_p] = D_c \left[1 - (1 - \frac{\alpha}{D_c})^{S_p + 1} \right]
\tag{3}
$$

$$
P_{B1}[bwin] = D_c \left[1 + \frac{(1 - D_c)}{D_c} (1 - \frac{\alpha}{D_c})^{bwin + 1} \right]
\tag{4}
$$

The collision probability defined as the probability of collision in at least one out of a total of S_p time slots is given as,

$$
P_C[S_p] = 1 - (1 - \alpha)^{S_p}
\tag{5}
$$

where $(1 - \alpha)^{S_p}$ represents the probability of the PU being in the on-state for S_p contiguous time steps. It is seen that the collision probability $P_C[S_p]$ depends only on α, and hence on the average off duration of the primary user. A symbolic representation of the steady state probability vector $\underline{\Pi}_Y : [\Pi_B, \Pi_{S_B}, \Pi_{T_x}, \Pi_{S_{T_x}}, \Pi_{R_{T_x}}, \Pi_{S_u}]^T$ as obtained from P_Y given in Eqn. 1 leads to the following probabilities,

$$
\Pi_B = \frac{P_{B0}[S_p]}{[2 * P_{B0}[S_p] - 3 * P_{B1}[bwin] + 3]}
\tag{6}
$$

$$
\Pi_{T_x} = \frac{1 - P_{B1}[bwin]}{[2 * P_{B0}[S_p] - 3 * P_{B1}[bwin] + 3]}
\tag{7}
$$

$$\Pi_{R_{T_x}} = \frac{P_C[S_p] * (1 - P_{B1}[bwin])}{[2 * P_{B0}[S_p] - 3 * P_{B1}[bwin] + 3]} \qquad (8)$$

$$\Pi_{S_u} = \frac{(1 - P_C[S_p]) * (1 - P_{B1}[bwin])}{[2 * P_{B0}[S_p] - 3 * P_{B1}[bwin] + 3]} \qquad (9)$$

with $\Pi_{S_B} = \Pi_B$ and $\Pi_{S_{T_x}} = \Pi_{T_x}$.

Examining the steady state probabilities, it is seen that the dependence on D_c arises from the terms $P_{B0}[S_p]$ and $1 - P_{B1}[bwin]$. From Eqns. 6-8, one can obtain the system parameters that satisfy specified performance constraints. For example, if the ratio of retransmission to transmission rate $\Pi_{R_{T_x}}/\Pi_{T_x}$ is to be bounded by $\epsilon_{R_{T_z}}$, the relation between α and S_p can be derived from 7 and 8 as,

$$\alpha = \frac{1}{T_{off}} = 1 - (1 - \epsilon_{R_{T_x}})^{\frac{1}{S_p}} \qquad (10)$$

If the ratio $\Pi_{T_x}/\Pi_B = \gamma_{T_x}$ of the transmit and backoff state probabilities is to be constrained, the backoff window size that can achieve this can be obtained as a function of the duty cycle and the packet size parameters as,

$$bwin = \frac{\ln[(\frac{D_c}{1-D_c}) * [\frac{1}{D_c} - \gamma_{T_x} * [1 - (1 - \frac{\alpha}{D_c})^{S_p}] - 1]]}{\ln(1 - \frac{\alpha}{D_c})} \qquad (11)$$

3. THROUGHPUT ANALYSIS FOR SECONDARY USERS

An important performance parameter is the throughput of the secondary user and the variability of this metric with parameters S_p and $bwin$ for a specified D_c. Given the secondary user dynamics through Y_n, the mean time taken to transmit a secondary user packet successfully is derived. The number of visits to the backoff and transmit states before exiting through the success state determines the time spent in successful transmission of a SU packet. To enable this computation, the state S_u is taken to be an absorbing state in a modified Markov chain $\hat{Y}_n$. The corresponding transition probability matrix $\boldsymbol{P}_{\hat{Y}}$ is,

$$
\begin{array}{c}
\begin{array}{cccccc}
B & S_B & T_x & S_{T_x} & R_{T_x} & S_u
\end{array} \\
\begin{array}{c}
B \\ S_B \\ T_x \\ S_{T_x} \\ R_{T_x} \\ S_u
\end{array}
\left(
\begin{array}{cccccc}
0 & 1 & 0 & 0 & 0 & 0 \\
P_{B1}[bwin] & 0 & 1 - P_{B1}[bwin] & 0 & 0 & 0 \\
0 & 0 & 0 & 0 & P_C[S_p] & 1 - P_C[S_p] \\
P_{B0}[S_p] & 0 & 1 - P_{B0}[S_p] & 0 & 0 & 0 \\
0 & 0 & 0 & 1 & 0 & 0 \\
0 & 0 & 0 & 0 & 0 & 1
\end{array}
\right)
\end{array} \qquad (12)
$$

In this representation, the five states $B, S_B, T_x, S_{T_x}, R_{T_x}$ are the transient states and S_u is the absorbing state.

The matrix $\boldsymbol{P}_{\hat{Y}}$ can be represented in terms of the matrix of transient states $\boldsymbol{Q}_{5x5}$ and vector $\boldsymbol{R}_{5x1}$ with elements that are one-step probabilities of reaching the absorbing state from each of the transient states.

$$\mathbf{P}_{\hat{Y}} = \begin{pmatrix} \mathbf{Q} & \mathbf{R} \\ \mathbf{0} & \mathbf{1} \end{pmatrix} \qquad (13)$$

where

$$\mathbf{Q} = \begin{array}{c} \\ B \\ S_B \\ T_x \\ S_{T_x} \\ R_{T_x} \end{array} \begin{array}{ccccc} B & S_B & T_x & S_{T_x} & R_{T_x} \\ \left(\begin{array}{ccccc} 0 & 1 & 0 & 0 & 0 \\ P_{B1}[bwin] & 0 & 1 - P_{B1}[bwin] & 0 & 0 \\ 0 & 0 & 0 & 0 & P_C[S_p] \\ P_{B0}[S_p] & 0 & 1 - P_{B0}[S_p] & 0 & 0 \\ 0 & 0 & 0 & 1 & 0 \end{array}\right) \end{array}$$

$$\mathbf{R} = \begin{array}{c} B \\ S_B \\ T_x \\ S_{T_x} \\ R_{T_x} \end{array} \begin{array}{c} S_u \\ \left(\begin{array}{c} 0 \\ 0 \\ 1 - P_C[S_p] \\ 0 \\ 0 \end{array}\right) \end{array}$$

with $\mathbf{0}_{1x5}$ and $\mathbf{1}_{1x1}$ containing zero and unit element values respectively.

The n-step transition probabilities of $\boldsymbol{P}_{\hat{Y}}$ are,

$$\mathbf{P}^n_{\hat{Y}_n} = \begin{pmatrix} \mathbf{Q}^n & \sum_{i=0}^{n-1} \mathbf{Q}^i \, \mathbf{R} \\ \mathbf{0} & \mathbf{1} \end{pmatrix} \qquad (14)$$

In the limit as $n \to \infty$, $\boldsymbol{Q}^n \to 0$ and $\sum_{i=0}^{\infty} \boldsymbol{Q}^i = \boldsymbol{N} = (\boldsymbol{I} - \boldsymbol{Q})^{-1}$.

The elements of matrix $\boldsymbol{N}$ have particular significance for computing the average time before absorption starting from a particular transient state. The ij^{th} element of $\boldsymbol{N}$, n_{ij} represents the expected number of visits to state j, starting from state i prior to absorption. Consider $\boldsymbol{N} = \boldsymbol{Q}^o + \boldsymbol{Q}^1 + \boldsymbol{Q}^2$ .... The ij^{th} element of $\boldsymbol{Q}^n$ given by $(q_{ij})^n$ represents the probability of transitioning to state j at the nth transition starting from an initial state i. Let V_{ij} be a positive valued random variable that represents the number of visits to state j from state i. The occupancy of state j can take place at the $1^{st}, 2^{nd}, 3^{rd}, ..., n^{th}$ transition. The random variable $(V_{ij})^n$ takes a value of one if the process transitions to state j from state i at the nth transition and zero otherwise. The probability that $(V_{ij})^n = 1$ is $(q_{ij})^n$. The expected number of transitions to state j from state i can be represented as

$$\begin{aligned} E[V_{ij}] &= \sum_{n=0}^{\infty} (0 \times P[V_{ij}^{(n)} = 0] + 1 \times P[V_{ij}^{(n)} = 1]) \\ &= \sum_{n=0}^{\infty} P[V_{ij}^{(n)} = 1] \\ &= \sum_{n=0}^{\infty} q_{ij}^{(n)} \end{aligned} \qquad (15)$$

Note that $E[V_{ij}]$ represents the element n_{ij} of matrix $\boldsymbol{N}$. Therefore, the sum of the elements in each row i of $\boldsymbol{N}$, provides the expected time before absorption starting from state i.

A symbolic calculation of $\boldsymbol{N}$ leads to the following expressions for each row, where the subscript signifies the starting state.

$$\mathbf{N} = \begin{pmatrix} \underline{N}_B \\ \underline{N}_{S_B} \\ \underline{N}_{T_x} \\ \underline{N}_{S_{T_x}} \\ \underline{N}_{R_{T_x}} \end{pmatrix} \qquad (16)$$

where,

$$\underline{N_B}^T = \begin{matrix} & B \\ B \\ S_B \\ T_x \\ S_{T_x} \\ R_{T_x} \end{matrix} \begin{pmatrix} \frac{P_{B0}[S_p]*P_C[S_p]-P_C[S_p]+1}{(1-P_{B1}[bwin])*(1-P_C[S_p])} \\ \frac{P_{B0}[S_p]*P_C[S_p]-P_C[S_p]+1}{(1-P_{B1}[bwin])*(1-P_C[S_p])} \\ \frac{1}{(1-P_C[S_p])} \\ \frac{P_C[S_p]}{(1-P_C[S_p])} \\ \frac{P_C[S_p]}{(1-P_C[S_p])} \end{pmatrix}$$

$$\underline{N_{S_B}}^T = \begin{matrix} & S_B \\ B \\ S_B \\ T_x \\ S_{T_x} \\ R_{T_x} \end{matrix} \begin{pmatrix} \frac{P_{B1}[bwin]+P_{B0}[S_p]*P_C[S_p]-P_{B1}[bwin]*P_C[S_p]}{(1-P_{B1}[bwin])*(1-P_C[S_p])} \\ \frac{P_{B0}[S_p]*P_C[S_p]+1}{(1-P_{B1}[bwin])*(1-P_C[S_p])} \\ \frac{1}{(1-P_C[S_p])} \\ \frac{P_C[S_p]}{(1-P_C[S_p])} \\ \frac{P_C[S_p]}{(1-P_C[S_p])} \end{pmatrix}$$

$$\underline{N_{T_x}}^T = \begin{matrix} & T_x \\ B \\ S_B \\ T_x \\ S_{T_x} \\ R_{T_x} \end{matrix} \begin{pmatrix} \frac{P_{B0}[S_p]*P_C[S_p]}{(1-P_{B1}[bwin])*(1-P_C[S_p])} \\ \frac{P_{B0}[S_p]*P_C[S_p]}{(1-P_{B1}[bwin])*(1-P_C[S_p])} \\ \frac{1}{(1-P_C[S_p])} \\ \frac{P_C[S_p]}{(1-P_C[S_p])} \\ \frac{P_C[S_p]}{(1-P_C[S_p])} \end{pmatrix}$$

$$\underline{N_{S_{T_x}}}^T = \begin{matrix} & S_{T_x} \\ B \\ S_B \\ T_x \\ S_{T_x} \\ R_{T_x} \end{matrix} \begin{pmatrix} \frac{P_{B0}[S_p]}{(1-P_{B1}[bwin])*(1-P_C[S_p])} \\ \frac{P_{B0}[S_p]}{(1-P_{B1}[bwin])*(1-P_C[S_p])} \\ \frac{1}{(1-P_C[S_p])} \\ \frac{1}{(1-P_C[S_p])} \\ \frac{P_C[S_p]}{(1-P_C[S_p])} \end{pmatrix}$$

$$\underline{N_{R_{T_x}}}^T = \begin{matrix} & R_{T_x} \\ B \\ S_B \\ T_x \\ S_{T_x} \\ R_{T_x} \end{matrix} \begin{pmatrix} \frac{P_{B0}[S_p]}{(1-P_{B1}[bwin])*(1-P_C[S_p])} \\ \frac{P_{B0}[S_p]}{(1-P_{B1}[bwin])*(1-P_C[S_p])} \\ \frac{1}{(1-P_C[S_p])} \\ \frac{1}{(1-P_C[S_p])} \\ \frac{1}{(1-P_C[S_p])} \end{pmatrix}$$

The expected time before absorption is obtained using the delay vector $\underline{D} = [bwin, 1, S_p, 1, 0]^T$ which assumes delay of one unit interval in the sensing states and delays of length $bwin$ and S_p

each time the process enters the backoff and transmit states respectively. After successful transmission, the process always starts from the S_{T_x} state. Therefore the expected time to reach the success state, denoted as τ can be calculated as follows:

$$\tau = \underline{N}_{S_{T_x}} \underline{D} \qquad (17)$$

The throughput, R_T for the secondary packet transmission with packet size S_p is therefore,

$$R_T = \frac{S_p}{\tau} \qquad (18)$$

The next section discusses the results and compares the theoretical model derived in this section with a simulation study.

4. THROUGHPUT ANALYSIS FOR SECONDARY USERS

In this section, the performance of sensing and transmission is analyzed for three duty cycles of the primary user: $D_c = 0.01, 0.1, 0.2$. The average off duration is fixed at $T_{off} = 100$ and T_{on} is determined using $D_c = T_{on}/(T_{on} + T_{off})$. The secondary packet size is nondimensionalized as $S_p^* = S_p/T_{off}$ and varied such that $0.01 \leq S_p^* \leq 1$. The nondimensionalized backoff window size is $bwin^* = bwin/T_{off}$. A simulation of the protocol is carried out to verify the theoretically derived steady state probabilities given in Eqns. (6-9). A discrete time simulation evolves the primary user in time n=1,2,... as a Markov process X_n, with $X_n = 0,1$ indicating channel free and occupied states. The SU is represented by the random process Y_n which is evolved in time using state dependent decisions based on the channel state and packet error conditions. The simulation is run for 10^5 successful packet transmissions. The model generated results are shown in solid lines and the simulation results are shown by symbols.

The variation of the transition probability $P_{B1}[bwin]$ given in Eqn. 4 as a function of D_c and $bwin^*$ is shown as a contour plot in Fig. 2. It can be seen that for low duty cycle, $P_{B1}[bwin]$ approaches a constant equal to D_c as the backoff window size is increased. To utilize this invariant feature, a backoff window size of $bwin^* = 2$ will be used, allowing one to approximate $P_{B1}[bwin] \approx D_c$ for the range of D_c considered.

Figs. [3-6] show the variation of the SU steady-state probabilities of being in the backoff, transmit, retransmit and success states respectively as a function of S_p^* with $bwin^* = 2$. The results are shown for $D_c = 0.01, 0.1$, and 0.2. The model and simulation results show a good agreement for all cases. The backoff probability Π_B increases with increase in duty cycle and becomes invariant for large values of S_p^*. As S_p^* increases, $P_{B0}[S_p]$ approaches D_c and $P_C[S_p]$ tends to unity from Eqn. 3 and 5 respectively. In this regime, $\Pi_B = \Pi_{S_B} = D_c/(2 * D_c + 3 * (1 - P_{B1}[bwin]))$. At 20% duty cycle the SU has 7% probability of being in the backoff state as S_p^* approaches one and thus equal to the average off duration of the PU, whereas this probability remains at 0.5% for $D_c = 0.01$ across the range of S_p^* considered.
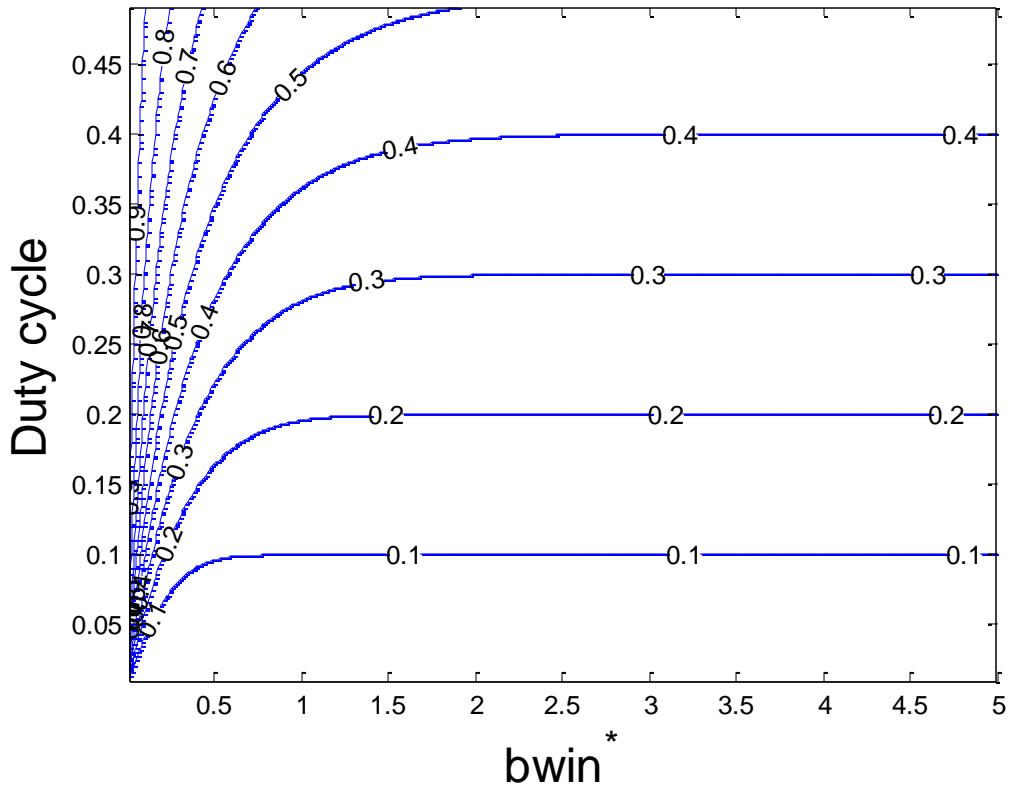
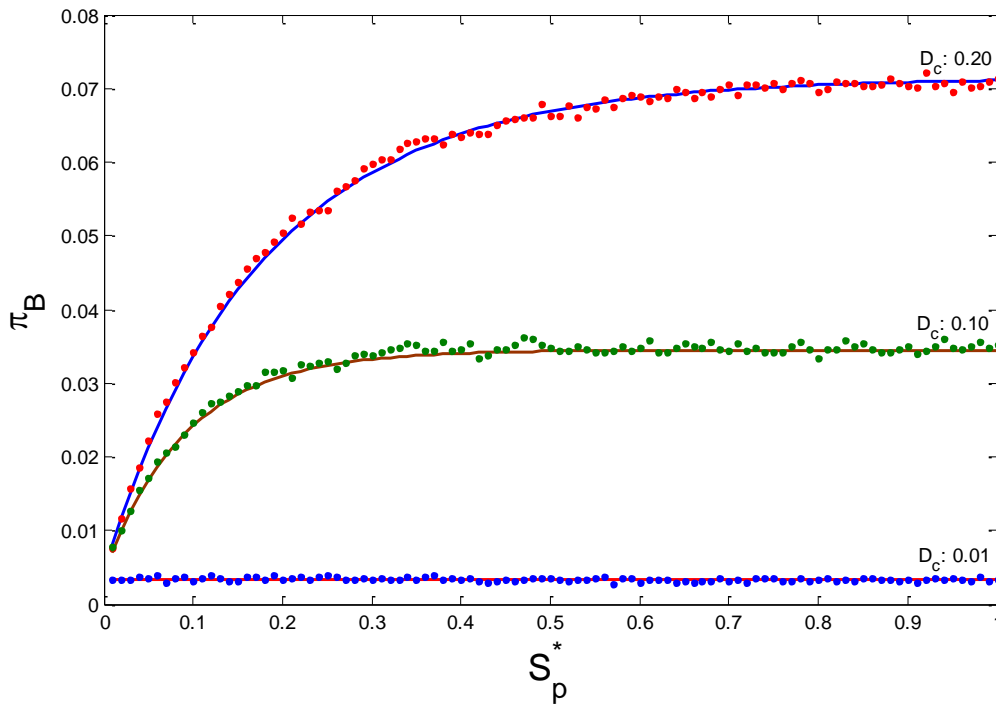**FIGURE 2:** Contour plots of $P_{B1}[bwin]$.
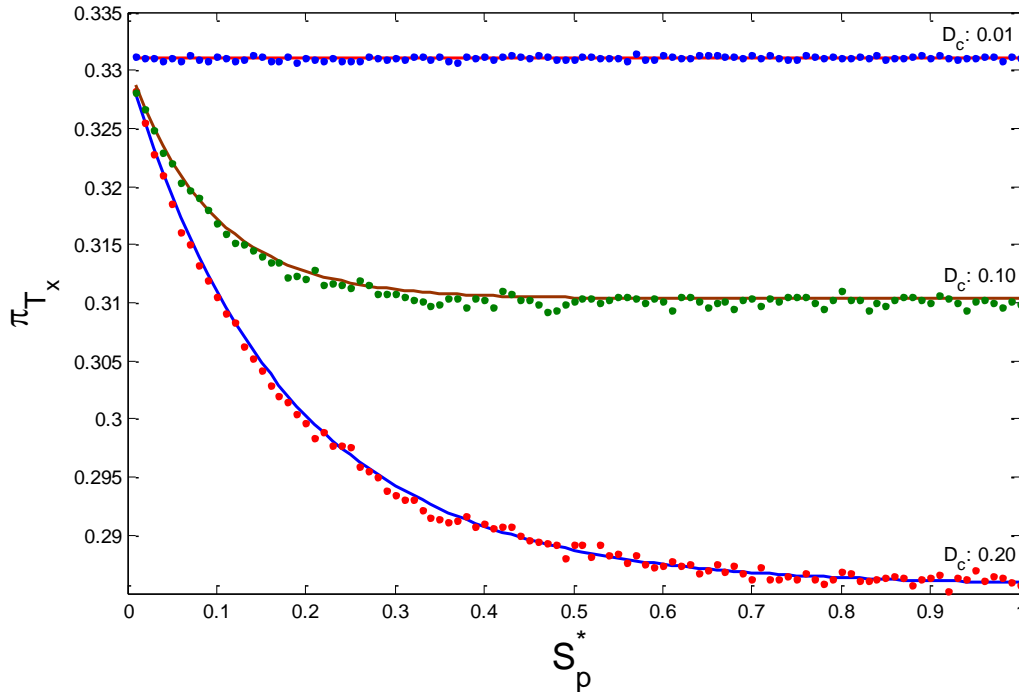

FIGURE 3: Analytical and simulation results for Π_B with fixed $bwin^* = 2$.

In Fig. 4 the probability Π_{T_x} of being in the transmit state is depicted for the three values of duty cycle and as a function S_p^*. This represents also the probability of being in the sense-after-transmit state $\Pi_{S_{T_x}}$. The level decrease in these probabilities as the duty cycle is increased results from the denominator term in Eqn. 8 which is a function of $P_{B0}[S_p]$ that increases with S_p, and $P_{B1}[bwin]$ is constant due to fixed $bwin^* = 2$. As the duty cycle increases, the secondary users will tend to enter the backoff state more often than the transmit state and hence the observed decrease in the transmission state probabilities. But it is important to note that because the probabilities of being in the backoff state are nearly an order of magnitude smaller than that of being in the transmit state, the dynamic range of the transmit probabilities as the duty cycle decreases from 0.2 to 0.01 is also quite small. For the parametric range considered, the SU operates around a thirty percent probability in the transmission state, and an equal probability of being in the sense after transmit state.

FIGURE 4: Analytical and simulation results for Π_{T_x} with fixed $bwin^* = 2$.

In Fig. 5, the probability of being in the retransmit state is depicted with change in the duty cycle. These probabilities decrease with an increase in the duty cycle for a fixed S_p^*, similar to the results for the transmission probability in Fig. 4. However, the retransmit probability for a fixed duty cycle increases with S_p^* due to increased number of packet errors from collision with the primary users, as the SU packet size increases. For small values, $S_p^* < 0.2$ the retransmit probability exhibits minimal sensitivity to the duty cycle.
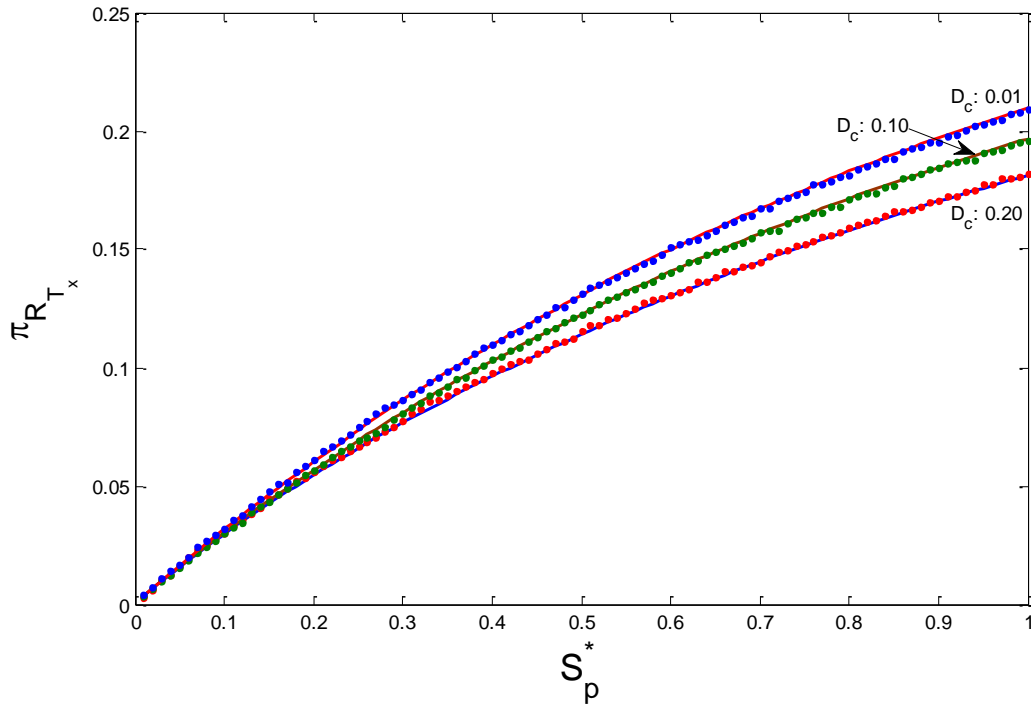
FIGURE 5: Analytical and simulation results for $\Pi_{R_{T_x}}$ with fixed $bwin^* = 2$.
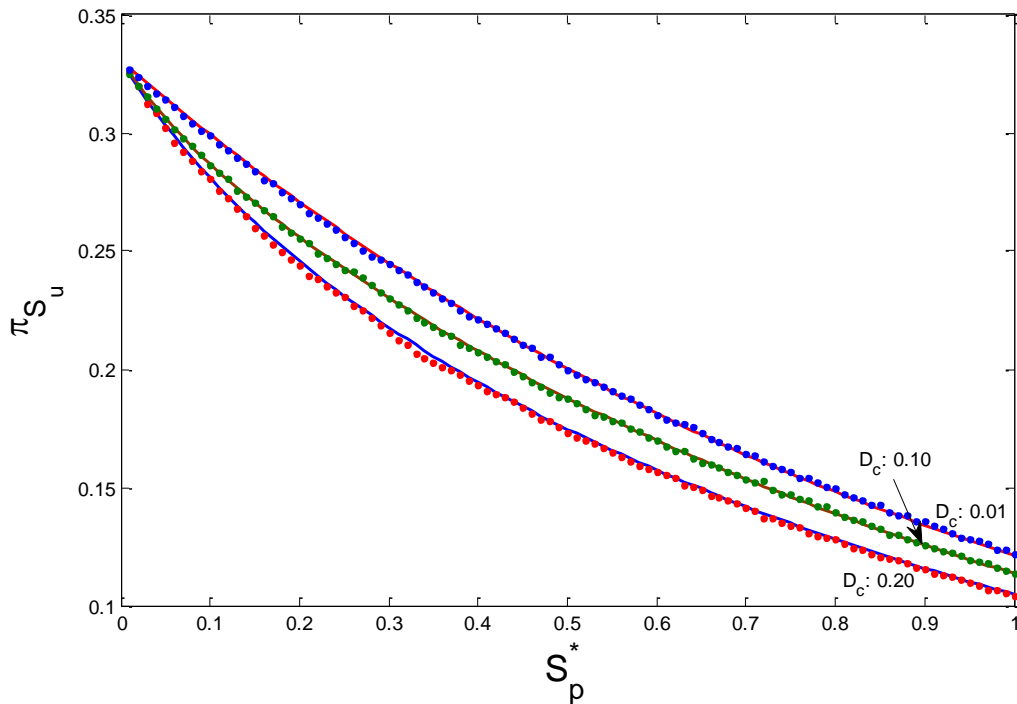

FIGURE 6: Analytical and simulation results for Π_{S_u} with fixed $bwin^* = 2$.

In Fig. 6, the probability of entering the success state decreases with an increase in the duty cycle and with increase in S_p^* and exhibits the most dynamic range among the state probabilities of the SU dynamics.
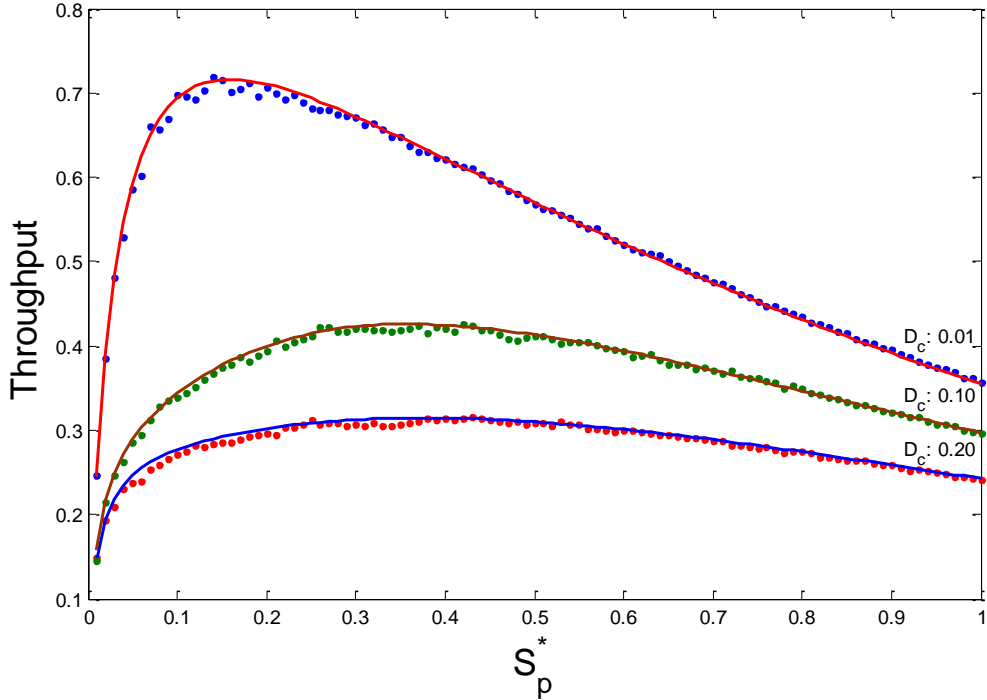
FIGURE 7: Analytical and simulation results for the secondary throughput with fixed $bwin^* = 2$.

The throughput calculated from simulation by estimating the average time taken for a successful packet transmission denoted as $\hat{\tau}$ is

$$\hat{R}_T = \frac{S_p}{\hat{\tau}} \qquad (19)$$

This is compared in Fig. 7 with the theoretical result R_T shown in Eqn. 18 for the range of duty cycles considered. A maximum throughput of 70% is observed at the lowest D_c of 0.01, the peak value occurring at a transmit frame size $S_p^* \approx 0.2$. With increase in D_c, the peak throughput decreases to 40% and 30% for D_c=0.1 and 0.2 respectively, while allowing the SU to operate at higher values of S_p^*.

5. THROUGHPUT ESTIMATION FOR RANDOM BACKOFF WINDOWS

In this section, the backoff window is taken to be a random variable drawn from uniform and exponential probability distributions with expected values equal to T_{off}. For the case of uniformly distributed window sizes, $bwin$ ranges from 0 to $4*T_{off}$ and in the case of an exponential distribution $bwin$ ranges from 0 to ∞. When the SU enters the backoff state (B), it randomly selects a waiting period drawn from the prescribed distribution. The other parameters such as S_p^* and D_c are varied in the same way as for the fixed backoff case. The probability of collision with the primary transmission during the secondary transmit state ($P_C[S_p]$) and the probability of the channel being busy after $S_p + 1$ transitions starting from an idle state ($P_{B0}[S_p]$) remain the same as in the case of the fixed backoff window. However, the probability of the channel being busy after $bwin + 1$ transitions starting from a busy state ($P_{B1}[bwin]$) now becomes a function of the random variable $bwin$.

The expected value of $P_{B1}[bwin]$, denoted as $\hat{P}_{B1}$ is applied in the transition probability calculation for the secondary user Markov chain, where,

$$\hat{P}_{B1_u} = \frac{1}{2*T_{off}} \int_{bwin=0}^{4*T_{off}} P_{B1}[bwin]d(bwin) \tag{20}$$

$$\hat{P}_{B1_e} = \frac{1}{2*T_{off}} \int_{bwin=0}^{\infty} P_{B1}[bwin]\, e^{-\frac{bwin}{2*T_{off}}} d(bwin) \tag{21}$$

The six-state model, the one-step transition probability matrix (P_Y) and the steady state probability vector, $\underline{\Pi}_Y : [\Pi_B, \Pi_{S_B}, \Pi_{T_x}, \Pi_{S_{T_x}}, \Pi_{R_{T_x}}, \Pi_{S_u}]^T$, remain the same as the fixed backoff window case except, for $P_{B1}[bwin]$ being replaced by $\hat{P}_{B1_r}[bwin]$.

Theoretically, the throughput is calculated by replacing $P_{B1}[bwin]$ with $\hat{P}_{B1_r}[bwin]$ in the fundamental matrix N given in Eqn. 16, and using the expected value $\widehat{bwin} = 2*T_{off}$ in the delay vector such that $\underline{D} = [\widehat{bwin}, 1, S_p, 1, 0]^T$.

The throughput resulting from fixed, uniform and exponentially distributed backoff windows is compared along with periodic sensing method. In periodic sensing, the channel is sensed at fixed intervals of $bwin$ for all S_p and D_c considered. If the channel is free, it transmits a packet $S_p < bwin$ and waits until the next sensing period $bwin - S_p$. If the channel is sensed busy, the waiting period is $bwin$.
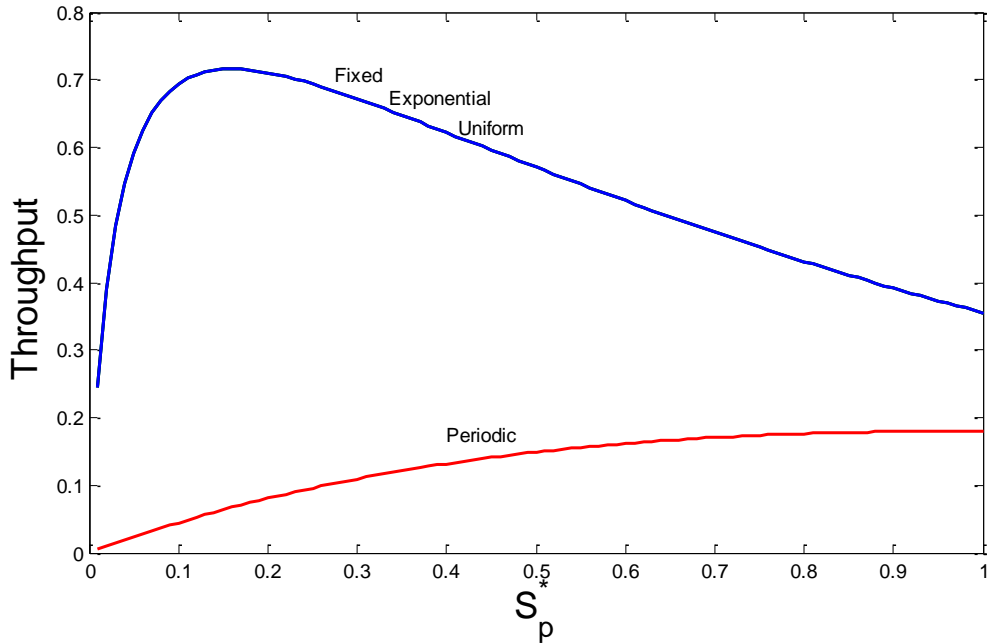

FIGURE 8: Analytical and simulation results for the secondary throughput for fixed, random and periodic backoff windows when $D_c = 0.01$ and $bwin^* = 2$.
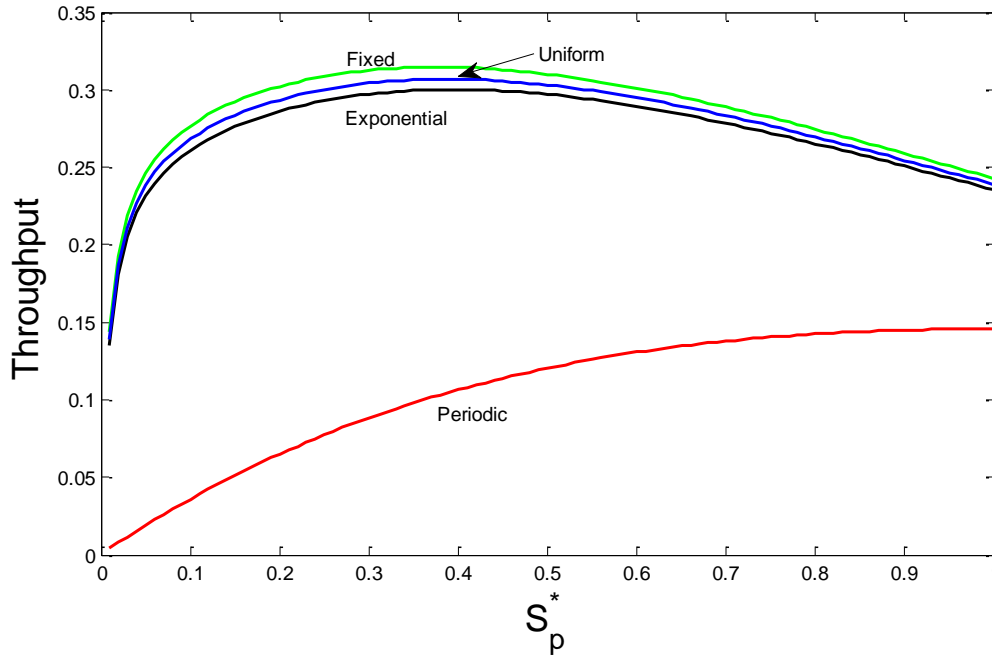
FIGURE 9: Analytical and simulation results for the secondary throughput for fixed, random and periodic backoff windows when $D_c = 0.20$ and $bwin^* = 2$.

Figs. 8 and 9 depict the SU throughput for the fixed, random and periodic backoff or sensing cases for $D_c = 0.01$ and $D_c = 0.20$ respectively. At the low PU duty cycle, random backoff windows have negligible effect on the throughput compared to a fixed $bwin$. As the duty cycle increases, for $D_c = 0.20$. The throughput due to random backoff windows decreases from the fixed backoff window model by about 5%. The asynchronous sensing generated by the proposed model is found to perform significantly better than the periodic sensing at $bwin^* = 2$, for which the peak throughput is reduced to less than twenty percent.

The combined effect of SU and PU parameters on the SU throughput can be visualized through contour plots of R_T as a function of S_p^* and $bwin^*$. Figs. 10, 11 and 12 depict the performance for duty cycles of 0.01, 0.10 and 0.20 respectively considering uniformly distributed backoff windows. These results show that SU throughput in the range of 70-80% can be achieved with $S_p^* < 0.35$ and $bwin^* < 5$ for $D_c = 0.01$. For $D_c = 0.10$ the operating region is reduced to $(S_p^*, bwin^*) < (0.3,1)$ and to $(S_p^*, bwin^*) < (0.3,0.5)$ for $D_c = 0.20$. Since S_p and $bwin$ are normalized with PU's T_{off}, increase in T_{off} reduces S_p^* and $bwin^*$ which results in higher SU's throughput verified using contour plots.
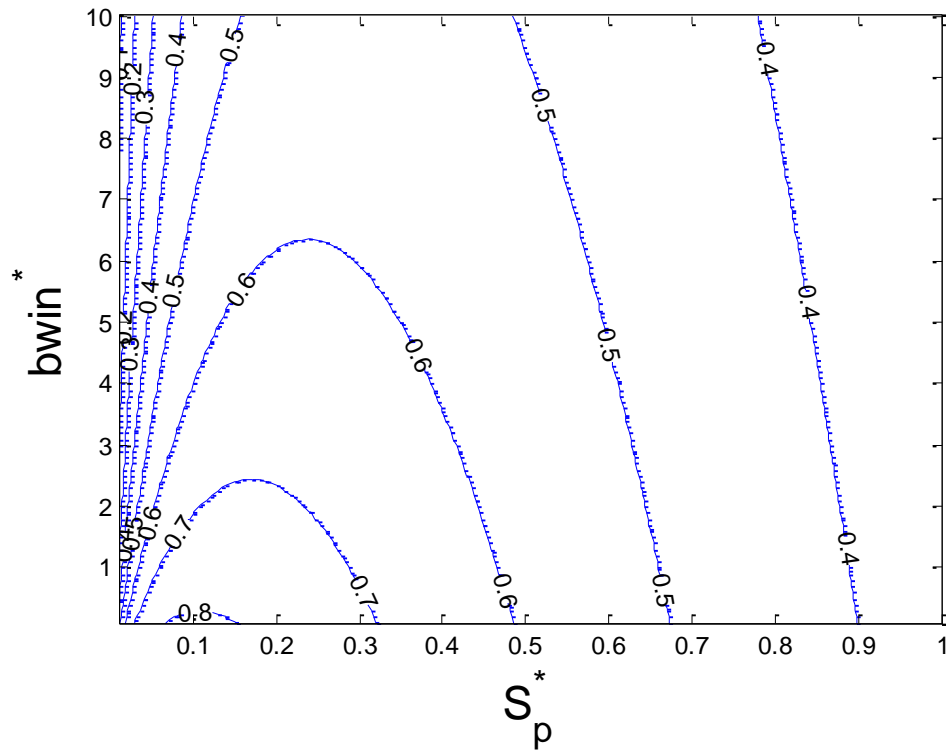
FIGURE 10: Contour plot of secondary throughput for primary duty cycle of 0.01.
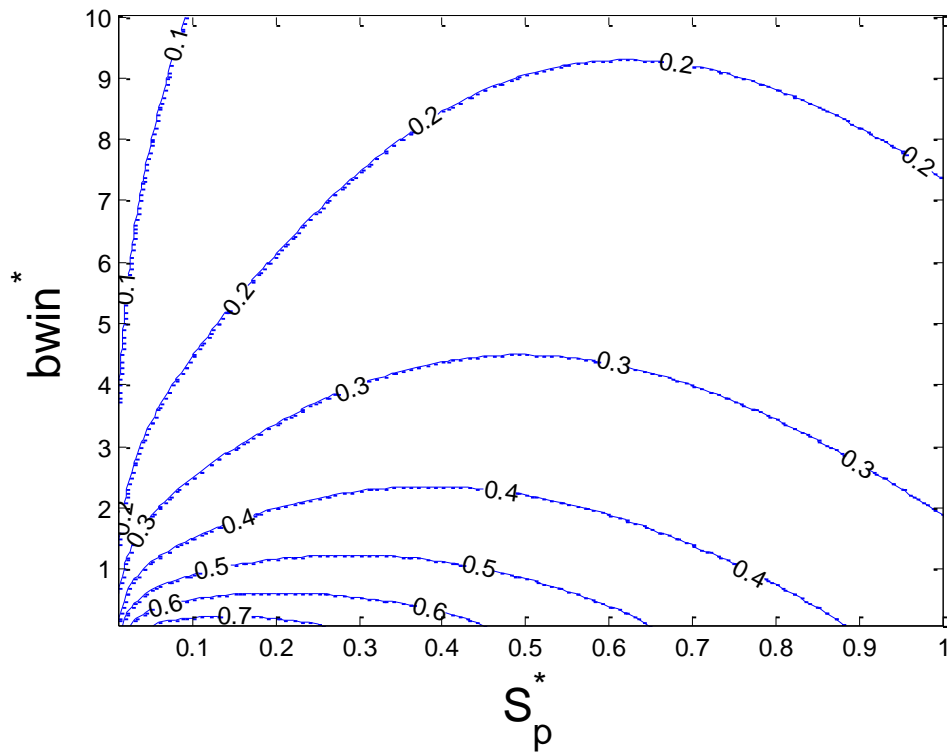

FIGURE 11: Contour plot of secondary throughput for primary duty cycle of 0.10.
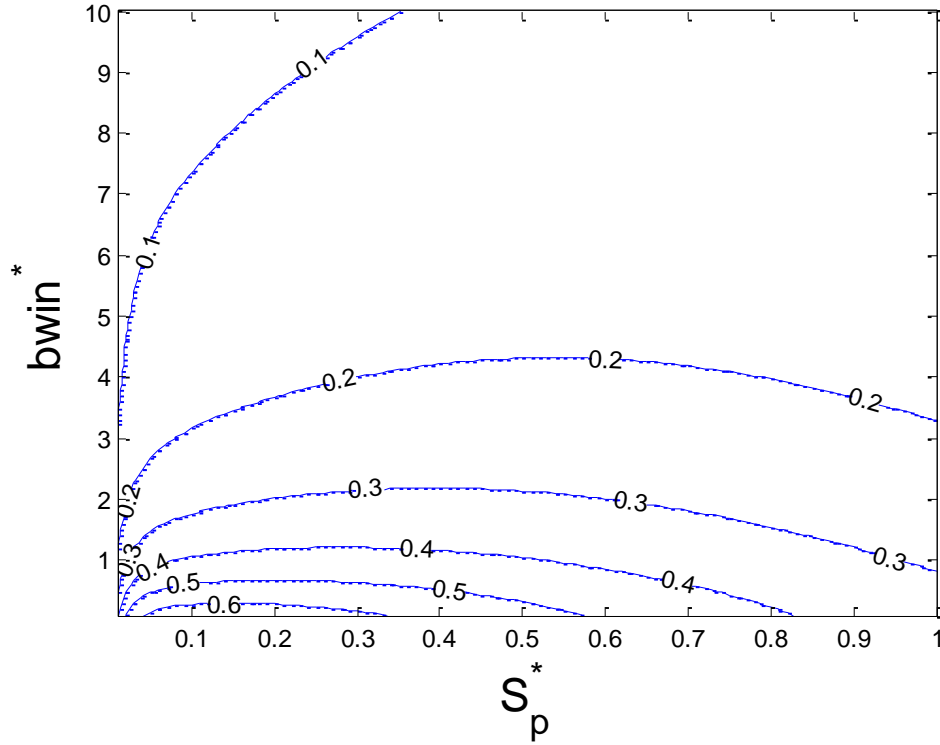
FIGURE 12: Contour plot of secondary throughput for primary duty cycle of 0.20.

Feasible operating regions in the space of (D_c, S_p^*) are identified so as to satisfy performance requirements such as: $\Pi_{T_x} > \Pi_B > \Pi_{R_{T_x}}$ and $\Pi_{R_{T_x}} < \Pi_{S_u}$. This ensures that collision with the primary is reduced, while ensuring that the quality of service to the secondary is maintained through the transmission probability. This performance is analyzed in the limit of large backoff window size $bwin$, which results in $P_{B1}[bwin] \approx D_c$ from Eqn. 4. This limit yields the following expressions for the backoff, transmission, retransmission and success probabilities,

$$\Pi_B = \frac{P_{B0}[S_p]}{2 * P_{B0}[S_p] - 3 * D_c + 3} \tag{22}$$

$$\Pi_{T_x} = \frac{1 - D_c}{2 * P_{B0}[S_p] - 3 * D_c + 3} \tag{23}$$

$$\Pi_{R_{T_x}} = \frac{P_C[S_p] * (1 - D_c)}{2 * P_{B0}[S_p] - 3 * D_c + 3} \tag{24}$$

$$\Pi_{S_u} = \frac{(1 - P_C[S_p]) * (1 - D_c)}{2 * P_{B0}[S_p] - 3 * D_c + 3} \tag{25}$$

In Figs. 13-15 a contour plot of $\Pi_B = \Pi_{T_x}$ is shown as a decreasing solid (red) line starting from the top left corner and $\Pi_B = \Pi_{R_{T_x}}$ is shown as an increasing solid (black) line starting from the bottom left corner with increasing S_p^*. These boundaries are derived from Eqns. 26 and 27 respectively. Eqn. 26 is from Eqns. 22 and 23, and Eqns. 22 and 24 yields Eqn. 27. The $\Pi_B = \Pi_{T_x}$ boundary delineates the constraint $\Pi_B > \Pi_{T_x}$ in the region above the red line and $\Pi_B < \Pi_{T_x}$ in the region below the red line. The black line $\Pi_B = \Pi_{R_{T_x}}$ also divides the space of (D_c, S_p^*) into regions

where $\Pi_B < \Pi_{R_{T_x}}$ below the line and $\Pi_B > \Pi_{R_{T_x}}$ above the line. The vertical green line, which is independent of D_c as per Eqn. 28 represents the case where $\Pi_{S_u} = \Pi_{R_{T_x}}$ derived from Eqns. 24 and 25 which yield Eqn. 28. On the left side of this line, $\Pi_{S_u} > \Pi_{R_{T_x}}$, and on the right side $\Pi_{S_u} < \Pi_{R_{T_x}}$. Thus the feasible operating region as per the performance constraints is in the region bounded by three contours and the vertical axis.

$$S_p = \frac{ln(\frac{2*D-1}{D})}{ln(1-\frac{\alpha}{D})} \qquad (26)$$

$$\frac{1-P_{B1}[bwin]}{D} = \frac{1-(1-\frac{\alpha}{D})^{S_p}}{1-(1-\alpha)^{S_p}} \qquad (27)$$

$$S_p = \frac{ln(\frac{1}{2})}{ln(1-\alpha)} \qquad (28)$$

FIGURE 13: Contours of Π_B and $\Pi_{R_{T_x}}$ and operating regions bounded by $\Pi_B = \Pi_{T_x}$ and $\Pi_B = \Pi_{R_{T_x}}$ with $bwin^* = 2$.
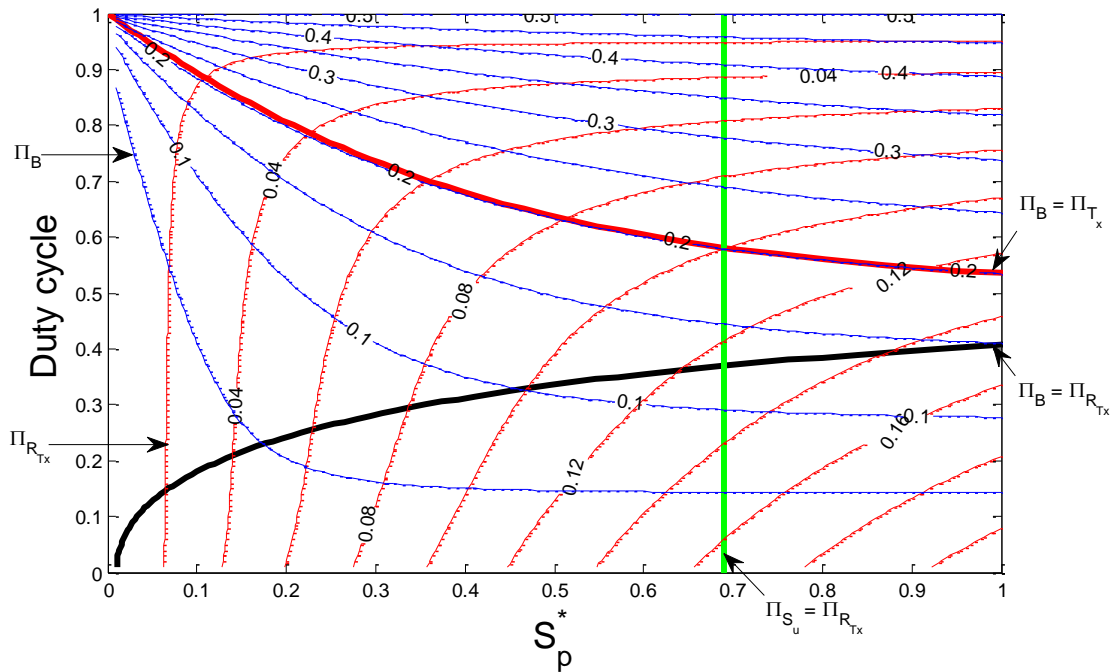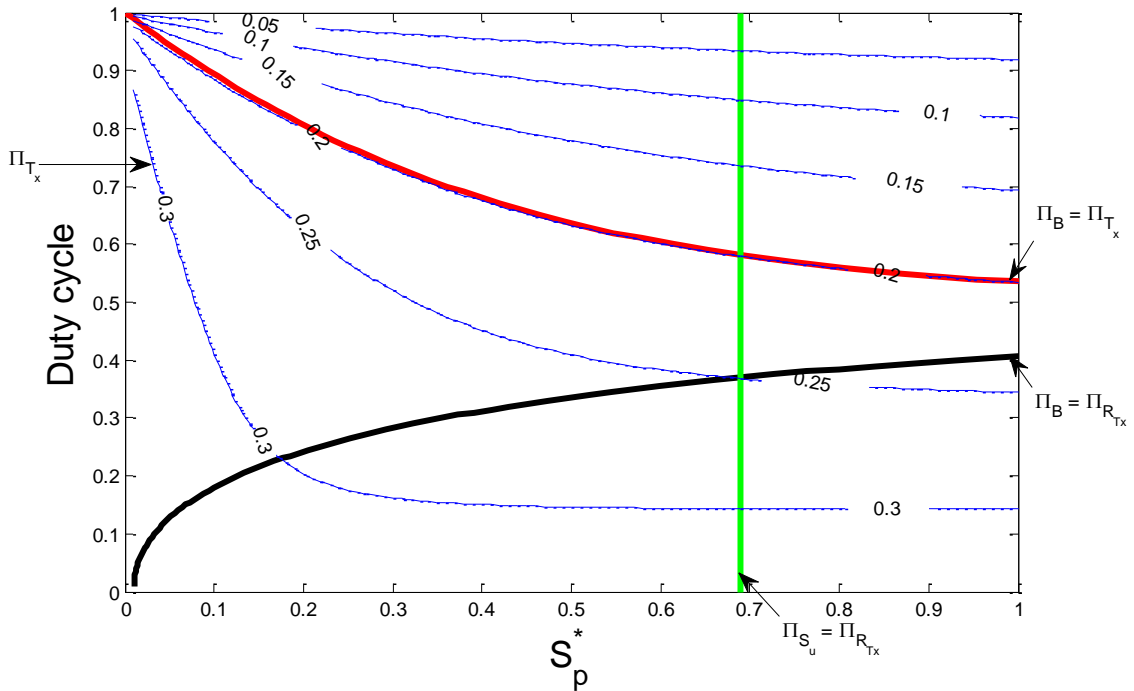
FIGURE 14: Contour of and Π_{T_x} and operating regions bounded by $\Pi_B = \Pi_{T_x}$ and $\Pi_B = \Pi_{R_{T_x}}$ with $bwin^* = 2$.
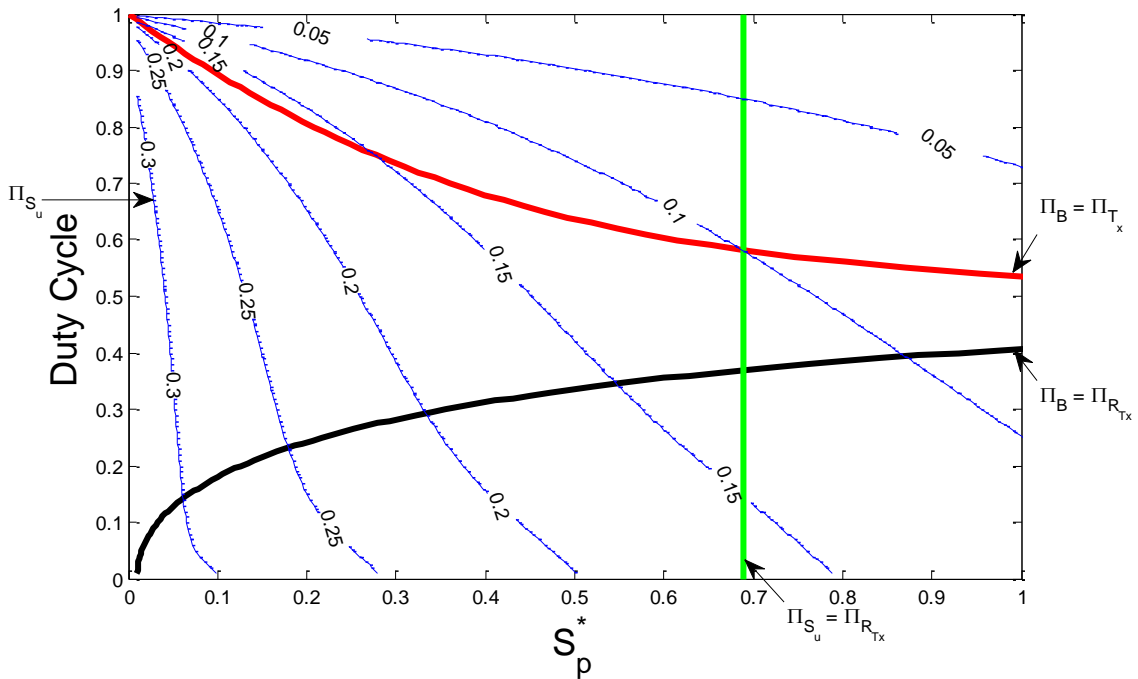

FIGURE 15: Contour of and Π_{S_u} and operating regions bounded by $\Pi_B = \Pi_{T_x}$ and $\Pi_B = \Pi_{R_{T_x}}$ with $bwin^* = 2$.

From the results shown in Fig. 13, 14 and 15, one can determine the operating regions of D_c and S_p^* that will satisfy the given performance metrics.

6. PERFORMANCE FOR TWO COOPERATIVE SECONDARY USERS

This section examines the throughput when two secondary users are in contention for the PU channel. A uniformly distributed backoff window is considered to demonstrate the effect. The analysis is carried out by simulation. The two SU's operate according to the aforementioned six state Markov model. If a channel is occupied either by the PU or another SU, the SU attempting to transmit enters the backoff state. On detection of collision after the transmit state, the SU will transition to the retransmit and the sense states. The simulation tracks the successful transmission of 10^5 packets by each of the secondary users. Fig. 16 compares the simulated throughput as a function of S_p^* for one and two SUs for $D_c = 0.01$ and $\widehat{bwin}^* = 1$. The peak SU throughput drops from 75% to about 20%. This study has assumed that the SU's generate a continuous stream of packets for transmission. Therefore the results shown correspond to the worst case scenario where no statistical multiplexing takes place during the channel access phase of the SU's.
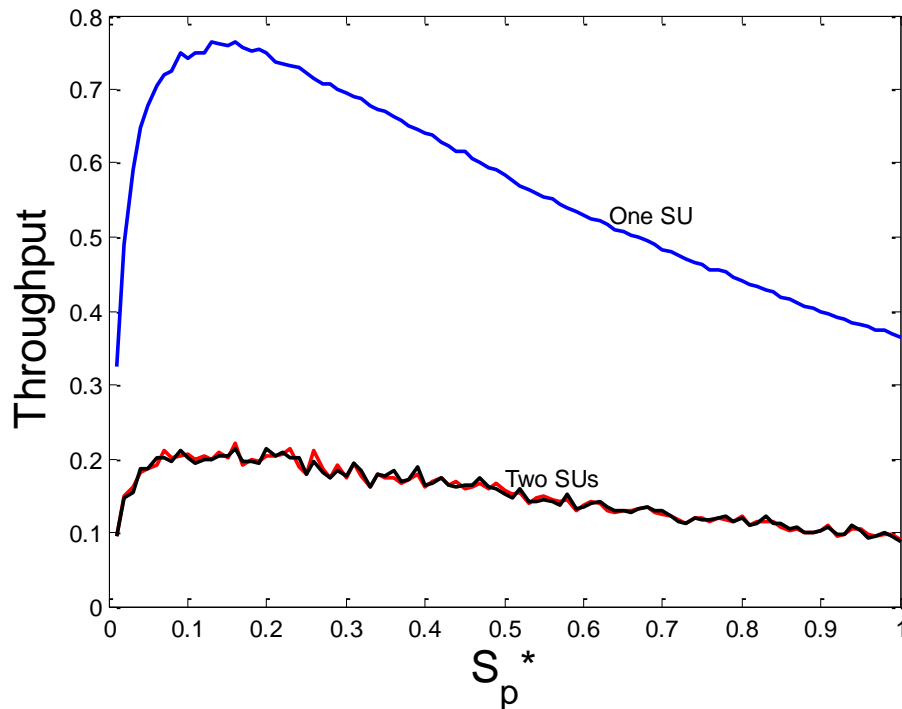

FIGURE 16: Throughput simulation for two cooperative secondary users for $D_c = 0.01$.

7. PERFORMANCE WITH A NON-COOPERATIVE SECONDARY USER

The effect on a SU's throughput is also analyzed for the case where a non-cooperative user (MU) attempts to access and block the channel for the SU while avoiding interference to a primary user. Both SU and MU actions are represented using the six state Markov model. In this case, the SU backs off when the channel is occupied either by the PU or MU. However, the MU avoids interference by the PU by sensing its presence and backing off, but ignores transmissions of the SU. The transmission frame size and backoff window size of the MU are varied to examine the impact on the SU throughput. Fig. 17 compares the SU throughput with and without the presence of the MU. The simulation results shown are for a PU duty cycle $D_c = 0.01$ with SU $\widehat{bwin}^* = 1$ and $0.01 < S_p^* < 0.50$. The packet size S_p of the MU does not affect the SU throughput performance if its backoff window is high enough so that it operates in the saturation regime shown in Fig. 2 where $P_{B1}[bwin]$ is invariant with S_p. This feature is seen in Fig. 17 where the SU throughput is obtained for MU $S_p = 1, 25, 50$ time units. The decrease in SU throughput is shown as the MU backoff window size is varied as $100 * T_{off}, 10 * T_{off}, 1 * T_{off}$. These results indicate that a non-cooperative user can operate covertly with small packet sizes, avoid detection from the primary

but significantly impact the performance of an opportunistic secondary user attempting to share the spectrum with a PU.
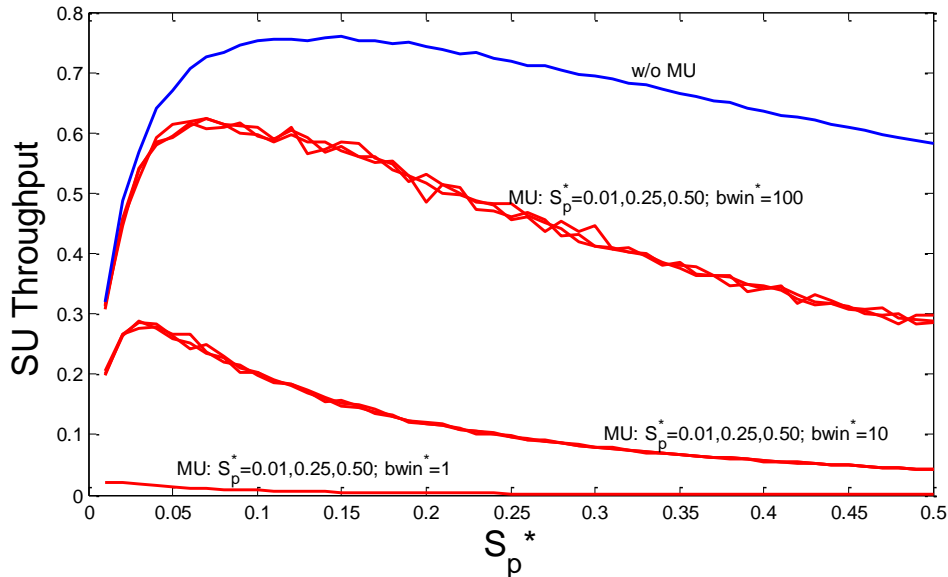

FIGURE 17: Throughput of SU with varying MU's $S_p^* = 0.01, 0.25, 0.50$, $bwin^* = 1, 10, 100$, and PU's $D_c = 0.01$.

The results in Fig. 17 assumed that the MU transmitted a packet with probability $p_{MU} = 1$ when the channel was sensed free of the PU. The MU can increase the degree of covertness by transmitting with probability $p_{MU} < 1$. Fig. 18 demonstrates the sensitivity of the SU throughput for $p_{MU} = 0.1$ and 0.5. The case for $p_{MU} = 1$ is also shown for comparison. The duty cycle is retained at $D_c = 0.01$ and the MU backoff window is $100 * T_{off}$. The SU throughput for all cases will be invariant if its transmission frame size $S_p^* < 0.05$, in which region the throughput is increasing with transmission frame size and in this region the presence of the MU can go undetected. However, as p_{MU} is increased from 0.1 to 1.0, the peak value is smaller and the decrease in the throughput is distinct for the different values of p_{MU}. In this regime of S_p, one can detect the presence of the MU, even at low values of p_{MU}.
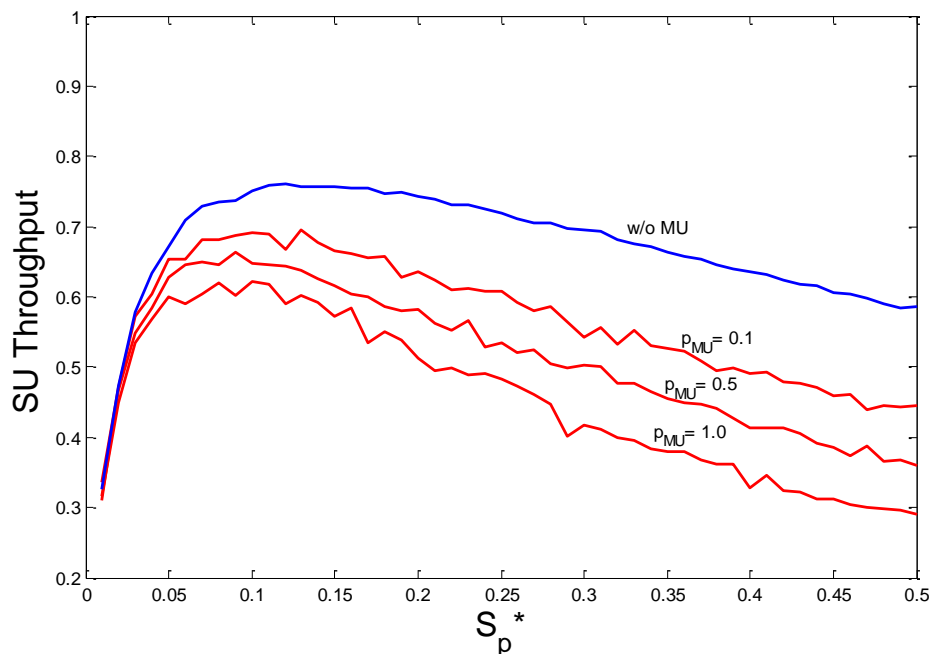
FIGURE 17: Simulated Throughput of SU with $p_{MU} = 0.1, 0.5, 1.0$ with $bwin^* = 100$, $D_c = 0.01$.

8. CONCLUSIONS

A joint sensing and transmission model is investigated for secondary users sharing spectrum with a primary user. The sensitivity of the SU probabilities of being in a transmit, retransmit or backoff states has been analyzed with respect to the PU duty cycle and average duration that the PU does not occupy the channel. A theoretical model for the SU throughput identifies the feasible operating region with respect to the SU packet length and backoff window size that leads to the peak throughput model for a specified PU duty cycle. The model is also shown to identify the range of PU duty cycles and SU transmission durations that maintain specified bounds on the probabilities of the SU being in the backoff and retransmit states. The model can be extended to multiple secondary users, with examples given here for the case of two cooperative and non-cooperative channel access.

9. ACKNOWLEDGEMENTS

10. REFERENCES

[1]   President Obama, "Presidential Memorandum-Expanding America's Leadership in Wireless Innovation." Internet: http://www.whitehouse.gov/the-press-office/2013/06/14/, June 14 2013 [Nov. 20, 2013].

[2]   President's Council of Advisors on Science and Technology, "Report to the President-Realizing the Full Potential of Government-held Spectrum to Spur Economic Growth," July 2012.

[3]   E. Axell, G. Leus, E.G. Larsson, and H.V. Poor, "Spectrum Sensing for Cognitive Radio," IEEE Signal Processing Magazine, vol. 29, pp.1315–1329, 2012.

[4]   Y.-E. Lin, K.-H. Liu, and H.-Y. Hsieh, "On using interference-aware spectrum sensing for dynamic spectrum access in cognitive radio networks," IEEE Transactions on Mobile Computing, vol. 12, pp. 461–474, March 2013.

[5]   D. Treeumnuk and D. Popescu, "Adaptive Sensing for Increased Spectrum Utilization in Dynamic Cognitive Radio Systems," in IEEE Radio and Wireless Symposium (RWS), 2012, pp. 319–322.

[6]   J. Deaton, C. Wernz, and L. DaSilva, "Decision analysis of dynamic spectrum access rules," in IEEE Global Telecommunications Conference (GLOBECOM), 2011, pp. 1–6.

[7]   L. Shi, K. W. Sung, and J. Zander, "Secondary spectrum access in tv-bands with combined co-channel and adjacent channel interference constraints," in IEEE International Symposium on Dynamic Spectrum Access Networks (DYSPAN), 2012, pp. 452–460.

[8]   M. Barrie, S. Delaere, G. Sukareviciene, J. Gesquiere, and I. Moerman, "Geolocation database beyond tv white spaces? matching applications with database requirements," in IEEE International Symposium on Dynamic Spectrum Access Networks (DYSPAN), 2012, pp. 467–478.

[9]   IEEE Std 802.22, "IEEE Standard for Information Technology–Telecommunications and information exchange between systems Wireless Regional Area Networks (WRAN)– Specific requirements Part 22: Cognitive Wireless RAN Medium Access Control (MAC) and Physical Layer (PHY) Specifications: Policies and Procedures for Operation in the TV Bands." IEEE Std 802.22-2011, 2011.

[10] M. Hamid, A. Mohammed, and Z. Yang, "On Spectrum Sharing and Dynamic Spectrum Allocation: MAC Layer Spectrum Sensing in Cognitive Radio Networks," International Conference on Communications and Mobile Computing (CMC), pp. 183-187, 2010.

[11] X. Wang, W.Chen, and Z. Cao, "Partially observable Markov decision process-based MAC-layer sensing optimization for cognitive radios exploiting rateless-coded spectrum aggregation," Communications, IET, vol. 6, pp. 828-835, 2012.

[12] K. Chang, Y. C. Huang, and B. Senadji, "Analysis of primary user duty cycle impact on spectrum sensing performance," in International Symposium on Information Theory and its Applications (ISITA), pp. 940–945, 2010.

[13] W. Gabran, C.-H. Liu, P. Pawelczak, and D. Cabric, "Primary user traffic estimation for dynamic spectrum access," IEEE Journal on Selected Areas in Communications, vol. 31, pp. 544–558, 2013.

[14] H. Kim and K. Shin, "Efficient discovery of spectrum opportunities with mac layer sensing in cognitive radio networks," IEEE Transactions on Mobile Computing, vol. 7, pp. 533–545, 2008.

[15] S. Zheng, Y.-C. Liang, P.-Y. Kam, and A.T. Hoang, "Cross-Layered Design of Spectrum Sensing and MAC for Opportunistic Spectrum Access," IEEE Conference on Wireless Communications and Networking (WCNC), pp. 1-6, 2009.

[16] C. Cormio and K. R. Chowdhury, "A Survey on MAC Protocols for Cognitive Radio Networks," ELSEVIER Ad Hoc Networks, vol. 7, pp. 1315–1329, 2009.

[17] W.-Y. Lee and I. Akyildiz, "Optimal spectrum sensing framework for cognitive radio networks," IEEE Transactions on Wireless Communications, vol. 7, pp. 3845–3857, 2008.

[18] Y. Pei, A.T. Hoang, and Y.-C. Liang, "Sensing-throughput tradeoff in cognitive radio networks: How frequently should spectrum sensing be carried out?," IEEE 18th International Symposium on Personal, Indoor and Mobile Radio Communications (PIMRC), pp. 1–5, 2007.

[19] P. Wang, L. Xiao, S. Zhou, and J. Wang, "Optimization of detection time for channel efficiency in cognitive radio systems," in IEEE Wireless Communications and Networking Conference (WCNC), pp. 111–115, 2007.

[20] P. Gandhi, I. Alshawabkeh, K. Chandra, and C. Thompson, "A spectrum sensing and transmission model for secondary users in cognitive radios," 20th International Conference on Software, Telecommunications and Computer Networks (SoftCOM), p.1-5, 2012.

[21] D. Cox and H. Miller, The Theory of Stochastic Processes, Methuen & Co Ltd., London, 1965.